The Interaction of V_2O_5 with TiO_2(Anatase): Catalyst Evolution with Calcination Temperature and O-Xylene Oxidation

RAMZI Y. SALEH,* ISRAEL E. WACHS,[1] SHIRLEY S. CHAN,[2] AND CLAUDIO C. CHERSICH

*Corporate Research–Science Laboratories, Exxon Research and Engineering Company, Annandale, New Jersey 08801, and *Intermediates Technology Division, Exxon Chemical Company, Baton Rouge, Louisiana 70821*

The interaction of V_2O_5 with the surface of TiO_2(anatase) was studied over the temperature range 110–750°C. The V_2O_5/TiO_2(anatase) system was characterized with laser Raman spectroscopy, X-ray photoelectron spectroscopy, Fourier transform infrared, X-ray diffraction, thermal gravimetric analysis, BET, and catalytic performance for o-xylene oxidation to phthalic anhydride. The state of V_2O_5/TiO_2(anatase) possessing high loadings of vanadia is strongly dependent on calcination temperature. In the presence of vanadia the TiO_2(anatase) support exhibits a simultaneous loss in surface area and structural transformation to rutile at elevated calcination temperatures. The morphology of the supported vanadia phase also depends on calcination temperature. At low calcination temperatures, 110–200°C, the vanadia exists as vanadyl oxalate, the starting vanadia salt. At intermediate calcination temperatures, 350–575°C, vanadia is present as a complete monolayer of surface vanadia species coordinated to the titania support and V_2O_5 crystallites. At calcination temperature of 575°C and above, the supported vanadia phase reacts with the TiO_2(anatase) support to yield $V_xTi_{1-x}O_2$(rutile). These structural changes have a pronounced effect on the catalytic performance of V_2O_5/TiO_2(anatase) catalysts for the oxidation of o-xylene. The optimum catalytic performance is observed for prolonged calcination at intermediate temperatures, 350–575°C, where a complete monolayer of surface vanadia exists on the TiO_2(anatase) support. The complete monolayer of surface vanadia and crystalline vanadia phases remain intact during the o-xylene oxidation reaction and become partially reduced by the reaction environment. © 1986 Academic Press, Inc.

INTRODUCTION

Many recent studies have shown that V_2O_5 supported on TiO_2 (anatase) is a superior catalyst than unsupported V_2O_5 for the selective oxidation of many hydrocarbons (1–9). These studies have revealed that TiO_2(anatase) modifies the properties of the supported vanadia phase by forming a monolayer of surface vanadia species coordinated to the TiO_2 support as well as small crystallites of V_2O_5 (5–11). The relative amount of surface vanadia and crystalline V_2O_5 depends on the vanadia content and the surface area of the TiO_2 support. The surface vanadia was found to be the active

site for the partial oxidation of hydrocarbons (5–9) and to possess a higher activity and selectivity than crystalline V_2O_5 for many hydrocarbon oxidation reactions. Moderate amounts of crystalline V_2O_5 do not significantly affect the catalytic performance of V_2O_5/TiO_2(anatase) because of the low effective surface area and poor catalytic activity of this phase.

At elevated temperatures the presence of the supported vanadia phase initiates the transformation of the titania support from anatase to rutile (3, 10–15). During this transformation the vanadia phase is reduced and becomes incorporated into the titania support as $V_xTi_{1-x}O_2$(rutile) (3, 10–15). The vanadia in solid solution with titania is stabilized as tetravalent vanadium (13, 15). Vejux and Courtine have proposed

[1] To whom all correspondence should be addressed.
[2] Present address: Technical Center, The BOC Group 100 Mountain Ave. Murray Hill, N.J. 07974

that the phase transformation from anatase to rutile and reduction of V$_2$O$_5$ are due to a remarkable fit of the crystallographic structures in contact at the interface between V$_2$O$_5$ and TiO$_2$(anatase) (*14*). Gasior *et al.* showed that these structural transformations unfavorably affect the activity and selectivity toward partial oxidation products during *o*-xylene oxidation over V$_2$O$_5$/TiO$_2$ (anatase) catalysts (*12*). To better understand the influence of calcination temperature upon the interaction of V$_2$O$_5$ with the surface of TiO$_2$(anatase), this supported oxide system was studied over the temperature range 110–750°C. The V$_2$O$_5$/TiO$_2$(anatase) samples were characterized with laser Raman spectroscopy (LRS), X-ray photoelectron spectroscopy (XPS), X-ray diffraction (XRD), diffuse reflectance infrared Fourier transform (DRIFT), thermal gravimetric analysis (TGA), and catalytic performance for *o*-xylene oxidation to phthalic anhydride.

EXPERIMENTAL

The TiO$_2$(anatase) was obtained from Mobay Corporation, and possessed a surface area of ~9 m^2/g. The TiO$_2$(anatase) support was found to contain 0.15 wt% K, 0.10 wt% P, 0.10 wt% Al, and 0.16 wt% Si as determined by atomic absorption. The presence of K and P on the surface of the TiO$_2$(anatase) was confirmed by XPS measurements. The 7 wt% V$_2$O$_5$/TiO$_2$ (anatase) catalysts were prepared by dissolving V$_2$O$_5$ in an aqueous solution of oxalic acid and impregnating the titania support. The excess water was allowed to evaporate at ~65°C. The catalysts were subsequently dried at 110°C and calcined in oxygen for 2 h at calcination temperatures from 200 to 750°C.

X-Ray diffraction patterns were obtained with a Philips diffractometer using Cu*K*α radiation and a diffracted beam monochromator. X-Ray diffraction examination confirmed that the fresh TiO$_2$(anatase) support did not contain any TiO$_2$(rutile). Lattice parameters were determined with the Least Squares Unit Cell Refinement Program of the Materials Research Laboratory of the Pennsylvania State University. BET measurements were performed with a Quantachrome Quantasorb using nitrogen.

X-Ray photoelectron spectroscopy measurements were made with a Leybold–Heraeus LHS-10 electron spectrometer. The X-ray source was obtained from an aluminum anode operated at 12 kV and 25 mA, and the binding energies of the V $2p_{3/2}$ signals were referenced to the Ti $2p_{3/2}$ peak at 458.5 eV (*16*).

A detailed description of the multichannel laser Raman spectrometer is given elsewhere (*17*). An argon ion laser (Spectra Physics, Model 165) was tuned to the 514.5-nm line for excitation. The laser power at the sample location was set at 40 mW. The Raman spectrometer was a triple monochromator (Instruments SA, Model DL203) that was coupled to an optical multichannel analyzer (Princeton Applied Research, Model OMA2). This optical multichannel analyzer system could deliver a spectrum about a factor of 100 faster than the conventional scanning spectrometer and averaging capability permitted measurements on samples of weak signals. The overall resolution was about 6 cm^{-1}.

The diffuse reflectance infrared Fourier transform (DRIFT) system is identical to the one previously described in the literature (*18*).

Thermal gravimetric analysis (TGA) was performed in a Mettler 2000C. The supported vanadia samples, ~100 mg, were first heated to 450°C in flowing oxygen, for approximately 1 h, to remove water vapor adsorbed on the samples. The samples were subsequently cooled to room temperature and the flowing oxygen stream was replaced by a flowing nitrogen stream. The sample was then heated at a rate of 10°C/min in the N$_2$ environment up to 900–1000°C.

The catalytic performance of the 7% V$_2$O$_5$/TiO$_2$(anatase) samples, calcined at different temperatures, for the oxidation of

o-xylene was examined in the reactor unit previously described (9). All catalysts were examined for this reaction with 1.25 mole% o-xylene in air, at a space velocity of 2760 h^{-1} and between 320 and 420°C. Air at the desired flow rate was passed through an o-xylene generator immersed in a temperature controlled water bath. A slip stream of the o-xylene/air feed was analyzed by a calibrated on-line multicolumn gas chromatograph equipped with a thermal conductivity detector. The gas chromatograph analyzed for all gases and organic components. After the desired o-xylene concentration was established, the feed was diverted to the reactor immersed in a molten salt (DuPont Hi Tech) bath. A slip stream of the reactor effluent was analyzed by the gas chromatograph for o-xylene conversions and the reaction products. The main reaction products observed were phthalic anhydride, tolualdehyde, phthalide, maleic anhydride, CO, CO_2 and water. Other products, including citraconic anhydride acid and benzoic acid, were ignored because they were present in very small quantities. At each temperature the reactor effluent was typically analyzed three to five times followed by several feed analyses. The carbon balance was always within 5%. The reactor was usually blanketed with N_2 during startup and overnight while the feed was being analyzed. The reactor (0.5-in. o.d., 316 stainless steel) was fitted with a 0.125-in. thermowell located at the center. A thermocouple inserted in the thermowell monitored the temperature throughout the catalyst bed. The feed was preheated to the salt bath temperature and entered the reactor from the bottom. The reactor was packed with 2 cm^3 of catalyst (corresponding to 1.96 g of V_2O_5/TiO_2(anatase) having a particle diameter of 0.4–0.7 mm) diluted with 8 cm^3 of 0.5-mm glass beads. This catalyst dilution ratio was found to give an isothermal profile along the length of the catalyst bed. The remaining reactor volume was filled with 3-mm glass beads (2 cm^3 at the top and 2 cm^3 at the bottom). Blank runs showed the reactor walls and beads to be inert with respect to o-xylene oxidation at the temperature range investigated.

RESULTS

X-Ray diffraction analysis showed that the state of the 7% V_2O_5/TiO_2(anatase) sample was strongly dependent upon the calcination temperature as shown in Table 1. The TiO_2(anatase) support did not undergo any phase transformations until a calcination temperature of 575°C. After the 575°C calcination treatment, a trace amount of the rutile phase was present. As the calcination temperature was further increased, the fraction of the rutile phase increased at the expense of anatase phase. Very little TiO_2 (anatase) remained in the sample after a calcination treatment of 750°C. In the absence of vanadia the TiO_2(anatase) support is stable and the rutile phase is not formed in this temperature range.

The rutile phase formed from 7% V_2O_5/ TiO_2(anatase) at high calcination temperatures, however, possessed lattice parameters slightly different from those of TiO_2(rutile) as shown in Table 2. Parameter c appears to be the same for TiO_2(rutile) and the rutile phase formed from 7% V_2O_5/ TiO_2(anatase) at high calcination temperatures. Lattice parameter a, however, is smaller for the rutile phase formed from 7%

TABLE 1

State of V_2O_5/TiO_2(Anatase) Catalyst Dependent on Calcination Temperature

Calcination temperature (°C)	XRD phases	
	V_2O_5	Rutile (%)
110	None	0
200	None	0
350	V. Weak	0
450	V. Weak	0
500	V. Weak	0
575	V. Weak	Trace
650	V. Weak	6
700	None	82
750	None	94

TABLE 2

Lattice Parameters for Rutile Phase Formed from
V₂O₅/TiO₂(Anatase) at High Calcination
Temperatures

Sample	Rutile (%)	a (Å)	c (Å)
TiO₂(rutile)	99.5	4.5954(2)	2.9599(2)
7% V₂O₅/TiO₂(A)—650°C	6	4.5906(4)	2.9603(6)
7% V₂O₅/TiO₂(A)—700°C	82	4.5899(3)	2.9590(5)
7% V₂O₅/TiO₂(A)—750°C	94	4.5913(7)	2.9599(10)

V₂O₅/TiO₂(anatase) than for TiO₂(rutile). The contraction of the rutile lattice for V₂O₅/TiO₂ samples heated to high temperatures has been attributed to the formation of a substitutional solid solution of V^{4+} in TiO₂(rutile) (3, 12). The formation of the rutile phase coincided with a change in color of the V₂O₅/TiO₂(anatase) samples from a light to a very dark color.

The kinetics of the vanadia–titania solid-state reaction at elevated temperatures were directly monitored with TGA experiments in a N₂ atmosphere as shown in Fig. 1 since the incorporation of vanadia into titania reduced V^{5+} to V^{4+}. (13, 15) The 7% V₂O₅/TiO₂ sample which was originally calcined at 450°C began to lose weight above 600°C due to the reduction of the vanadia and this solid-state reaction was complete at approximately 750°C. The evolution of oxygen and some water vapor originating from surface hydroxyls was observed during temperature-programmed experiments with a mass spectrometer downstream from the 7% V₂O₅/TiO₂ sample. The reduction of vanadia was not observed over the same experimental conditions when an α-Al₂O₃ support, ~12m²/g, was substituted for TiO₂(anatase), and demonstrates that this solid-state reaction is specific to TiO₂.

The state of the supported V₂O₅ phase in the 7% V₂O₅/TiO₂(anatase) sample was also dependent upon calcination temperature. Crystalline V₂O₅ was not present in the XRD patterns below calcination temperatures of 350°C and above calcination temperatures of 650°C. To obtain additional in-

formation about the state of the supported vanadia phase these samples were examined with laser Raman spectroscopy and infrared spectroscopy. The two techniques are complementary since the LRS has excellent sensitivity to the metal–oxygen vibrations of small V₂O₅ crystallites as well as noncrystalline vanadia phases (9, 10), and infrared spectroscopy has excellent sensitivity to carbon–oxygen vibrations in the vanadyl oxalate group (19).

The laser Raman spectra of unsupported V₂O₅ and TiO₂(anatase) in the range ~750–1250 cm⁻¹ were previously presented (9). Bulk V₂O₅ exhibits a sharp Raman peak at 997 cm⁻¹ which is associated with the symmetrical stretching mode of the terminal oxygen atom (V=O) (20); additional bulk V₂O₅ Raman bands lie below 750 cm⁻¹. The TiO₂(anatase) possesses a weak second-order feature at 794 cm⁻¹ in the same region; the major anatase Raman bands appear at 144, 199, 399, 520, and 643 cm⁻¹ (20). The diffuse reflectance infrared Fourier transform peak frequencies of unsupported V₂O₅ and TiO₂ (anatase) are presented in Table 3. Bulk V₂O₅ exhibits a sharp infrared peak at 1025 cm⁻¹ due to the stretching vibration of the terminal oxygen atom (V=O), and a broad infrared band at 850 cm⁻¹ due to the deformation vibration of V–O–V bridges (3). The TiO₂(anatase) IR spectrum possesses a broad band centered at ~750
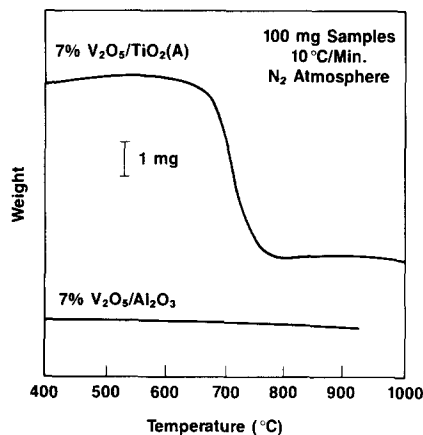

FIG. 1. Thermal gravimetric analysis of 7% V₂O₅/ TiO₂(anatase) and 7% V₂O₅/Al₂O₃ (alpha) samples.

TABLE 3

IR Peak Frequencies of Reference Materials

Sample	400–800 cm⁻¹	801–1200 cm⁻¹	1201–1400 cm⁻¹	1401–1800 cm⁻¹
TiO₂(anatase)	750(w)–broad[a]	—	—	1640(vw)
V₂O₅	—	850(m), 981(vw) 1025(s)	1200(vw), 1275(vw)	—
Oxalic acid dihydrate	490(m), 552(m), 718(s)	875(s), 920(s)	1230(s), 1302(m) 1400(s)	1482(m), 1730(s), 1770(sh)
Vanadyl oxalate	495(m), 543(m), 770(m)	805(s), 853(vw) 902(m), 931(vw) 942(VW), 982(s), 1060(w)	1270(m), 1315(m), 1358(w)	1405(s), 1435(s) 1595(sh), 1640(s), 1690(sh), 1710(sh)

[a] vw, very weak; w, weak; m, medium; s, strong; sh, shoulder.

cm^{-1}, and additional broad bands at ~1640 and ~3200 cm^{-1} due to the deformation vibrations of adsorbed water and surface hydroxyls (3). The infrared peak frequencies of unsupported oxalic acid and vanadyl oxalate, prepared from V_2O_5 and oxalic acid, are also shown in Table 3. The infrared peaks in the region 1200–1800 cm^{-1} are associated with the carbon–oxygen stretches in the oxalate group of oxalic acid and vanadyl oxalate (19). The strong IR band at 982 cm^{-1} is assigned to the vanadium–oxygen stretch of vanadyl oxalate, and is consistent with the metal–oxygen stretch of other metal oxalate compounds (19). Note that the IR peak frequencies of vanadyl oxalate are distinctly different from those of oxalic acid and crystalline V_2O_5, and reveal that these two reagents effectively reacted to form the vanadyl oxalate.

The laser Raman spectra of the 7% V_2O_5/ TiO₂(anatase) sample as a function of calcination temperature are presented in Fig. 2, and the corresponding IR data are shown in Table 4. Previous studies have shown that the 7% V_2O_5 on TiO₂(anatase) possessing ~9 m²/g corresponds to ~4–5 monolayers equivalent of V_2O_5 (5–10). However, following low calcination temperatures (110 and 200°C), the sharp crystalline V_2O_5 peak at 997 cm^{-1} is absent from the Raman spectra. Instead, there is a weak and broad Raman band suggestive of a noncrystalline

vanadia phase (9, 10). Diffuse reflectance infrared Fourier transform studies of the sample calcined at 110°C reveal strong absorption bands in the region 1400–1700 cm^{-1} which are due to the carbon–oxygen stretches of the oxalate groups in vanadyl oxalate and reveal that the deposited vana-
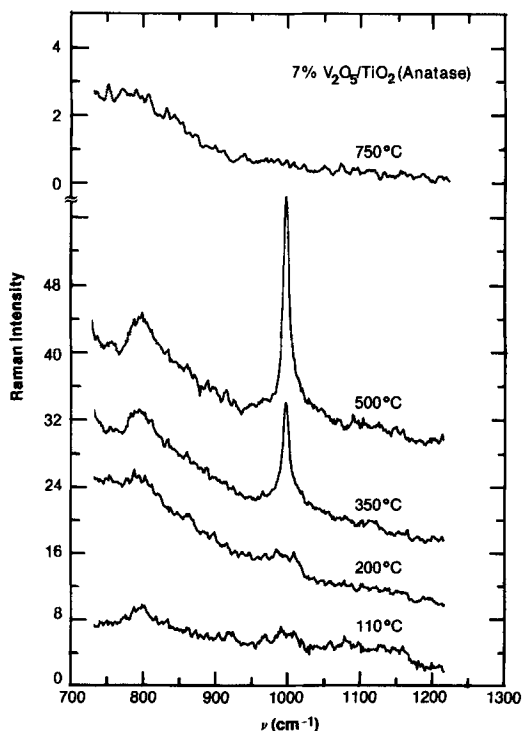

FIG. 2. Laser Raman spectra of 7% V_2O_5/TiO₂(anatase) as a function of calcination temperature.

TABLE 4

IR Peak Frequencies of Fresh 7% V$_2$O$_5$/TiO$_2$(Anatase) as a Function of Calcination Temperature

Calcination temperature (°C)	800–1200 cm^{-1}	1201–1400 cm^{-1}	1401–1800 cm^{-1}
110	950(w)–broad[a]	1270(w), 1315(w)	1415(s), 1685(s), 1715(sh)
350	1010(m)	—	1620(m)
450	1018(m)	—	1620(m)
575	1022(m)	—	1620(m)
650	1020(m)	—	1620(m)
700	—	—	1620(m)
750	—	—	1620(m)

[a] w, weak; m, medium; s, strong; sh, shoulder.

dyl oxalate is intact in this temperature range. The corresponding Raman data for the region 1200–2000 cm^{-1} do not possess any Raman features of the oxalate group because of the poor scattering properties of this group (19). As the calcination temperature is increased to 350°C, the infrared bands of vanadyl oxalate disappear, and a V$_2$O$_5$ peak appears at ~1010 cm^{-1} in the infrared spectrum and at 997 cm^{-1} in the Raman spectrum. The intensity of the crystalline V$_2$O$_5$ Raman peak increases as the calcination temperature is further increased. Crystalline V$_2$O$_5$ Raman bands at 704, 485, 307, and 287 cm^{-1} are also observed for these samples. After a calcination treatment of 750°C, the V$_2$O$_5$ peak is completely absent from the Raman spectrum and the infrared spectrum. The intensity of the 997 cm^{-1} Raman band is shown in Fig. 3 in greater detail as a function of calcination temperature. The intensity of this Raman band increases up to a calcination temperature of 450°C and decreases above calcination temperatures of 575°C.

The supported vanadia phase in the 7% V$_2$O$_5$/TiO$_2$(anatase) samples calcined at different temperatures was also examined with X-ray photoelectron spectroscopy. The XPS V 2p$_{3/2}$ binding energies of the 7% V$_2$O$_5$/ TiO$_2$(anatase) samples were found to be constant at 517.3–517.4 eV for samples calcined up to 650°C. This binding energy

corresponds to vanadium in the +5 oxidation state of V$_2$O$_5$ (21). The XPS V/Ti ratio, however, was found to strongly vary with calcination temperature as shown in Fig. 4. The XPS V/Ti ratio initially decreased as the calcination temperature was increased from 110 to 350°C, and subsequently increased as the calcination temperature was increased from 350 to 650°C. The BET surface area of the 7% V$_2$O$_5$/TiO$_2$(anatase) simultaneously decreased as the calcination
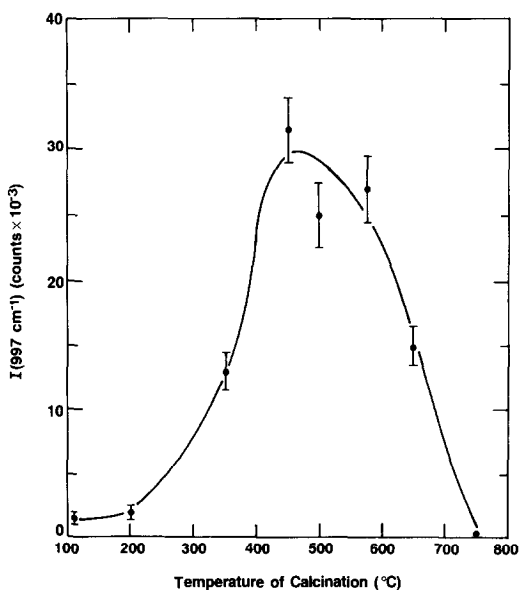

FIG. 3. Intensity of 997-cm^{-1} Raman band of 7% V$_2$O$_5$/TiO$_2$(anatase) as a function of calcination temperature.
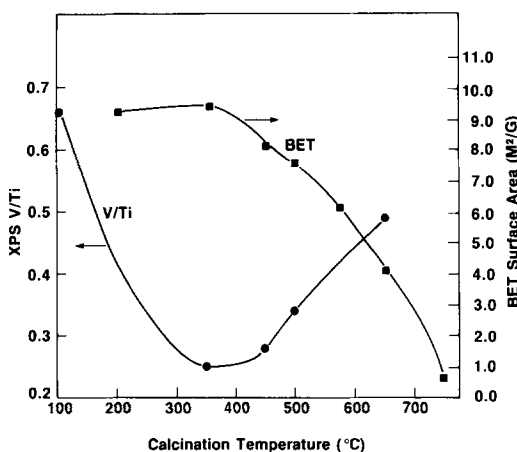
FIG. 4. BET surface area and XPS V/Ti ratio as a function of calcination temperature.

temperature was raised above 350°C (see Fig. 4). These XPS measurements further reveal that the morphology of the vanadia phase on the TiO_2 support varied with calcination temperature.

The 7% V_2O_5/TiO_2(anatase) samples which had been calcined at different temperatures were also examined for their catalytic performance for o-xylene oxidation as shown in Figs. 5a and b. The catalysts were generally operated at 340–360°C for approximately 1 to 2 days prior to taking the data presented in Figs. 5a and b. During this break-in period the o-xylene conversion increased ~5% and the selectivity increased ~1–2%. The activity and selectivity toward C_8-oxygenates (phthalic anhydride, phthalide, and o-tolualdehyde) of 7% V_2O_5/TiO_2(anatase) were strongly dependent upon the calcination temperature. The sample which had been calcined at 450°C was the most active for the oxidation of o-xylene, and the 350°C calcined sample was slightly less active. The uncalcined sample, 110°C pretreatment, was less active than the above samples for this reaction. The 700°C calcined sample exhibited a very low activity for o-xylene oxidation, and much higher temperatures were required to achieve significant conversion of o-xylene. Furthermore, unlike the other catalysts this catalyst was not stable and ex-

tensively deactivated with time on stream. The selectivity toward C_8-oxygenates of the sample calcined at 450°C was slightly higher than that of the sample calcined at 350°C, and that of the uncalcined catalyst, 110°C pretreatment, was slightly lower than the above. However, the C_8-oxygenate selectivity of the sample calcined at 700°C was very inferior, and substantial amounts of o-tolualdehyde and phthalide were present in the product stream. Thus, calcination temperature has a profound effect on the performance of V_2O_5/TiO_2(anatase) catalysts for the oxidation of o-xylene.

The 7% V_2O_5/TiO_2(anatase) samples were altered by the o-xylene oxidation reaction as previously discussed (22). Upon completion of the catalytic runs, the reactor was purged with nitrogen and removed from the salt bath at the reaction temperature. This removal procedure, as well as the subsequent handling in air, resulted in partial reoxidation of the used V_2O_5/TiO_2(anatase) catalysts. However, the used catalysts were still sufficiently altered by the o-xylene oxidation reaction that significant differences existed between the fresh and used catalysts. Analysis of the spent 7% V_2O_5/TiO_2(anatase) catalysts calcined at 350 and 450°C showed that the V_2O_5 crystallites originally present in the fresh catalysts, corresponding to the sharp 997 cm^{-1} Raman band, were reduced by the o-oxylene reaction to lower oxides of crystalline vanadium oxide, corresponding to the absence of the 997 cm^{-1} Raman band. The surface vanadia species coordinated to the TiO_2(anatase) support, however, were found to be oxidized in the spent V_2O_5/TiO_2 (anatase) catalysts. The surface vanadia was most probably also partially reduced by the o-xylene oxidation reaction, but was reoxidized by the ambient environment prior to characterization. The more facile oxidation of the surface vanadia is probably related to the fact that, unlike crystalline vanadia, every surface vanadia is exposed to the environment. The spent 7% $V_2O_5/$ TiO_2(anatase) catalyst calcined at 110°C did
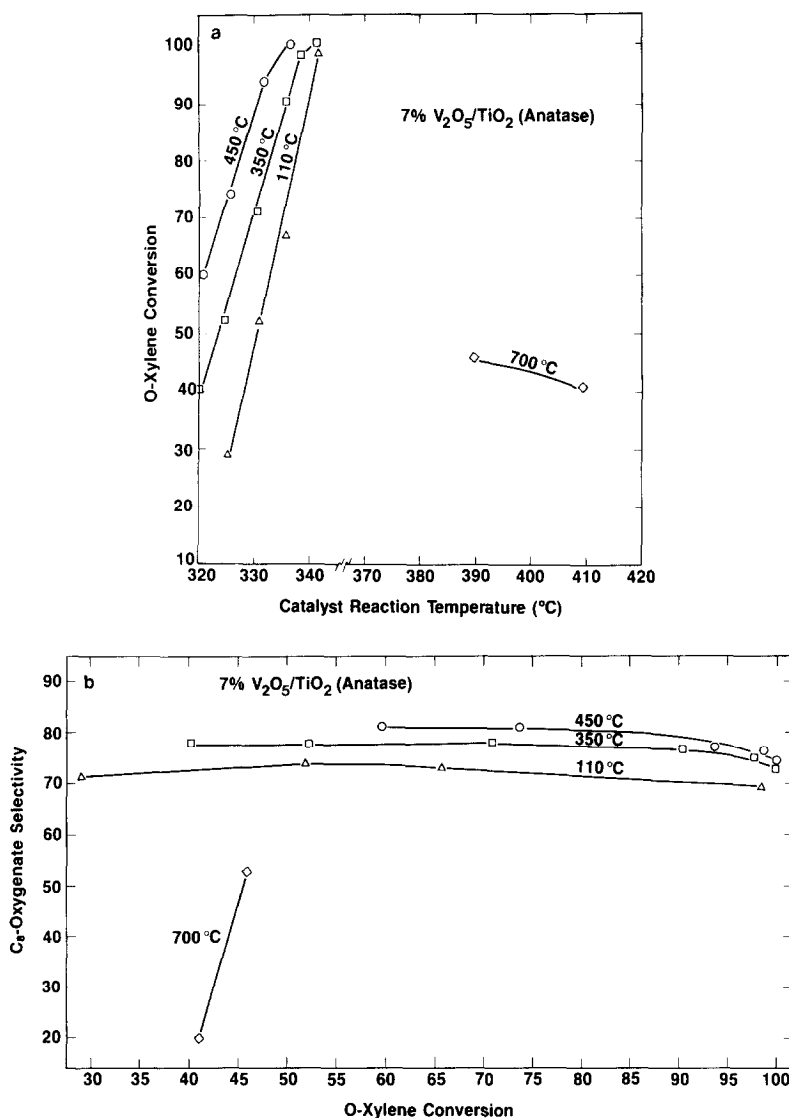
FIG. 5. (a) Conversion of *o*-xylene for the 7% V$_2$O$_5$/TiO$_2$(anatase) catalyst as a function of calcination temperature. (b) Selectivity toward C$_8$-oxygenates for the 7% V$_2$O$_5$/TiO$_2$(anatase) catalyst as a function of calcination temperature.

not possess the oxalate groups of vanadyl oxalate, which exhibits characteristic infrared bands at ~1400 and ~1700 cm^{-1}, and revealed that the oxalate groups decomposed during the conditions of the *o*-xylene oxidation reaction. Crystalline V$_2$O$_5$ was also not found in this spent catalyst. The 7% V$_2$O$_5$/TiO$_2$(anatase) catalyst calcined at 700°C did not possess crystalline V$_2$O$_5$ before and after the *o*-xylene oxidation reaction.

DISCUSSION

At elevated temperatures (575–750°C), and only in the presence of vanadia, the TiO$_2$(anatase) support exhibited a simultaneous loss in surface area and formation of a substitutional solid solution of V^{4+} in TiO$_2$(rutile), V$_x$Ti$_{1-x}$O$_2$. Bond *et al.* found that the maximum amount of vanadia incorporated in TiO$_2$(rutile) corresponds to V$_{0.04}$Ti$_{0.96}$O$_2$ (*3*). The formation of the solid

solution $V_xTi_{1-x}O_2$(rutile) is reflected in the contraction of the rutile lattice (see Table 2), because V^{4+} is slightly smaller than Ti^{4+} (*3, 12*), and weight loss of V_2O_5/TiO_2(anatase) samples in a N_2 environment at elevated temperatures during TGA experiments. Additional support for the formation of the vanadia–titania solid solution comes from extended X-ray absorption fine structure (EXAFS) (*11*) and ESR studies (*15*). The EXAFS spectrum beyond the vanadium K-edge of V_2O_5/TiO_2(anatase) heated to high temperatures exhibited the titanium K-edge of pure rutile (*11*), and ESR showed that about 90% of the vanadium is present in the form of V^{4+} ions that were resistant to oxidation (*15*). These changes are consistent with the change in sample color from light for the supported vanadia phase to very dark when the $V_xTi_{1-x}O_2$(rutile) phase was present.

The data presented demonstrate that the state of vanadia in V_2O_5/TiO_2(anatase) also strongly depends on calcination temperature. At low calcination temperatures, 110–200°C, the Raman, IR, and XRD data collectively reveal that the vanadia exists as noncrystalline vanadyl oxalate. The initially high XPS V/Ti ratio suggests that the supported vanadyl oxalate phase uniformly covers the TiO_2(anatase) surface. This situation is schematically shown in Fig. 6, 110–200°C, where several layers of vanadyl oxalate are present on the TiO_2(anatase) support. As the calcination temperature is further increased to 350°C the vanadyl oxalate decomposes as reflected in the disappearance of the oxalate infrared bands at ~1400 and ~1700 cm^{-1}. Simultaneously, the Raman and XRD data exhibit the presence of V_2O_5 crystallites, and the XPS V/Ti ratio is significantly reduced. These changes imply that the vanadia phase is beginning to agglomerate and crystallize as V_2O_5 as schematically depicted in Fig. 6, 350°C. Earlier Raman studies revealed that crystalline V_2O_5 formation occurs only after the TiO_2(anatase) surface is covered with a complete monolayer of the surface
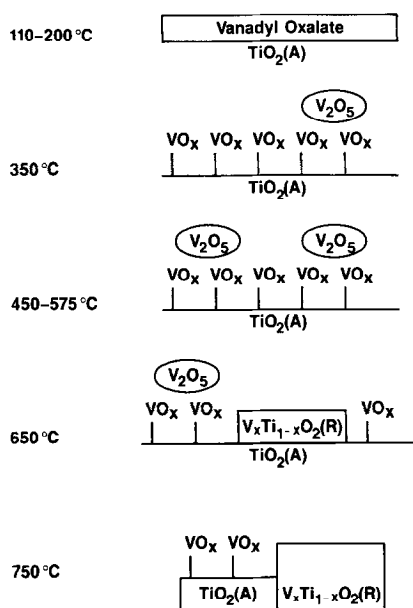

FIG. 6. Model of the evolution of V_2O_5/TiO_2 with calcination temperature.

vanadia species (*9*), and in the present case there is about three to four times V_2O_5 in excess of monolayer. Increasing the calcination temperature from 350 to 575°C leads to simultaneous changes in the supported vanadia phase and the TiO_2(anatase) support. In this temperature range the TiO_2(anatase) support experiences about a 30% loss in surface area, the Raman shows an increase in the content of crystalline V_2O_5, and the XPS V/Ti ratio increases. These changes suggest that the portion of vanadia present as crystalline V_2O_5 increases at the expense of the surface vanadia coordinated to the titania support as shown in Fig. 6, 450-575°C. Similar behavior was observed for the WO_3/Al_2O_3 system at elevated calcination temperatures when there was a significant loss in the surface area of the alumina support (*17*). As the surface area of the alumina support decreased a portion of the surface tungsten oxide species coordinated to the alumina was transformed to WO_3 crystallites (*17*). At 575°C the solid-state reaction between vanadia and TiO_2 (anatase) to form $V_xTi_{1-x}O_2$(rutile) is initiated as revealed by the appearance of a

trace of rutile in the XRD pattern. As the calcination temperature is further increased above 575°C the solid-state reaction between vanadia and TiO_2(anatase) is accelerated. After a 650°C calcination treatment approximately 6% of the titania is present as $V_xTi_{1-x}O_2$(rutile) and the crystalline V_2O_5 content is diminished (see Fig. 6, 650°C). The XPS measurements of the sample calcined to 650°C exhibited a V $2p_{3/2}$ binding energy consistent with V^{5+} and suggest that the surface concentration of $V_xTi_{1-x}O_2$(rutile), which contains V^{4+}, must be low. After a calcination treatment of 700–750°C crystalline V_2O_5 is not present in the Raman spectrum and most of the vanadia is incorporated into the titania support as $V_xTi_{1-x}O_2$(rutile). This situation is schematically depicted in Fig. 6, 750°C. Essentially, the same catalyst evolution was observed when vanadium ethoxide in ethanol was used instead of vanadyl oxalate in water as the starting vanadia material (23). Thus, the preparation method does not appear to influence the subsequent V_2O_5/TiO_2 interactions as the calcination temperature is increased.

The presence of crystalline V_2O_5 appears to be essential for the formation of $V_xTi_{1-x}O_2$(rutile) from the supported vanadia phase and TiO_2(anatase). Bond et al. reported that for TiO_2(anatase) possessing ~9 m^2/g the V_2O_5 content must be in excess of 2% for the transformation of TiO_2(anatase) into $V_xTi_{1-x}O_2$(rutile) (3). Our Raman studies have shown that for the 9 m^2/g titania, 2% V_2O_5 corresponds to approximately a monolayer of the surface vanadia species and crystalline V_2O_5 is only present in significant amounts in these V_2O_5/TiO_2(anatase) samples at higher vanadia loadings (9). The EXAFS studies of V_2O_5/TiO_2(anatase) heated to various temperatures by Kozlowski et al. showed that the monolayer of surface vanadia species was first converted to crystalline V_2O_5 prior to the formation of $V_xTi_{1-x}O_2$(rutile) (11). Additional laser Raman studies with high-surface-area V_2O_5/TiO_2 samples by the present

authors also demonstrated that the formation of the $V_xTi_{1-x}O_2$(rutile) phase occurs only in the presence of crystalline V_2O_5 on the titania support (23). Very similar behavior was also observed for supported WO_3 on Al_2O_3 (17, 24). At elevated temperatures the reaction between the supported tungsta phase and alumina to form $Al_2(WO_4)_3$ occurred only when crystalline WO_3 was present. Controlled-atmosphere electron microscopy studies of the behavior of the WO_3/Al_2O_3 system at high temperatures suggested that the solid-state reaction between the supported tungsta phase and the alumina to form $Al_2(WO_4)_3$ takes place by the transport of alumina from the support to the WO_3 crystallites (24). The very dramatic loss in surface area of the 7% V_2O_5/TiO_2 sample above 350°C suggests that vanadia catalyzes the mobility of titania since TiO_2(anatase) in the absence of vanadia is stable in this temperature range. Thus, the vanadia–titania solid-state reaction most likely also proceeds by the transport of titania to the V_2O_5 crystallites, and not by the penetration of the supported vanadia into the TiO_2(anatase) lattice.

Vejux and Courtine have proposed that the phase transformation from anatase to rutile and reduction of V_2O_5 have their origin in the remarkable fit of the crystallographic structures in contact at the interface between V_2O_5 and TiO_2(anatase) (14). All the available experimental data do suggest that the presence of crystalline V_2O_5 is required for these transformations to occur. The above hypothesis, however, does not take into account the disordered monolayer of surface vanadia present on the titania support (9–11). Thus, the two crystalline structures (V_2O_5 and TiO_2(anatase)) are not in direct contact, but are in contact with the amorphous surface vanadia monolayer. Furthermore, the formation of $V_xTi_{1-x}O_2$ (rutile) is not limited to TiO_2(anatase) supports as proposed by Vejux and Courtine, and also occurs with TiO_2(rutile) supports (3, 13, 23, 25).

The catalytic performance of 7% $V_2O_5/$

TiO$_2$(anatase) for o-xylene oxidation is markedly influenced by calcination temperature. Calcination at intermediate temperatures, 350–450°C, yields active and selective catalysts. Uncalcined catalysts, 110°C treatment, exhibit somewhat lower activity and selectivity, and calcination at high temperatures, 700°C, results in inferior catalysts for o-xylene oxidation. In the most active catalysts, 350 and 450°C calcination, the supported vanadia phase is present as vanadia crystallites and a complete monolayer of the surface vanadia species. Analysis of the spent V$_2$O$_5$/TiO$_2$(anatase) catalysts revealed that the monolayer of surface vanadia species and crystalline vanadia phases remain intact during the o-xylene oxidation reaction. The crystalline vanadia phase in the spent catalysts, however, is reduced by the reaction environment (22). Earlier studies demonstrated that the surface vanadia is more active and selective than the crystalline vanadia for the o-xylene oxidation reaction, and that the surface vanadia is the active site for this reaction (9). Thus, the reduction of the crystalline V$_2$O$_5$ phase to lower oxides under the reaction conditions should not impact on the activity and selectivity of the o-xylene oxidation reaction. The critical feature of the V$_2$O$_5$/TiO$_2$(anatase) catalysts is that the monolayer of surface vanadia remains intact during the o-xylene oxidation reaction environment. The observed catalytic performance of the sample calcined at 450°C is slightly better than that of the catalyst calcined at 350°C (see Figs. 5a and b). This slight difference may be due to the fact that at 350°C sintering of the crystalline vanadia phase is not complete and consequently some of the surface vanadia sites may be covered by crystalline vanadia somewhat more extensively in the 350°C calcined sample than the 450°C calcined sample.

The uncalcined catalyst, 110°C, exhibits a much lower activity and selectivity than the sample calcined at 450°C (see Figs. 5a and b). The morphology of the vanadia phase in the uncalcined sample is initially very different from that present in the calcined samples (see Fig. 6). Crystalline V$_2$O$_5$ is not present in the fresh uncalcined sample, and the high XPS V/Ti ratio reveals that vanadia is present as several uniform layers of vanadyl oxalate on the TiO$_2$(anatase) support. IR analysis of the spent uncalcined catalyst revealed that the vanadyl oxalate decomposed under the o-xylene oxidation reaction conditions. The lower catalytic activity of the uncalcined sample suggests that the agglomeration of the supported vanadia phase in excess of monolayer in this sample is probably incomplete under reaction conditions, and that a portion of the surface vanadia, the active site for o-xylene oxidation, is still covered by unsintered crystalline vanadia. The slightly lower selectivity of the uncalcined catalyst is probably a consequence of the direct participation of this unsintered crystalline vanadia component in the o-xylene oxidation reaction.

The V$_2$O$_5$/TiO$_2$(anatase) catalyst calcined at 700°C exhibits very inferior catalytic performance for o-xylene oxidation compared to the catalysts calcined at lower temperatures. In the 700°C calcined sample the supported vanadia phase is present as crystalline V$_x$Ti$_{1-x}$O$_2$(rutile) and as surface vanadia species coordinated to titania. Earlier studies demonstrated that the TiO$_2$(anatase) support must be covered by a complete monolayer of the surface vanadia species in order to be active and selective for the o-xylene oxidation reaction because exposed titania sites lead to complete combustion of the partial oxidation products (8, 9). The substantial decrease in the selectivity toward C$_8$-oxygenates of the V$_2$O$_5$/TiO$_2$ catalyst calcined at 700°C suggests that a complete monolayer of the surface vanadia is not present on the titania support after a calcination temperature of 700°C. For the 700°C sample, most of the vanadia is apparently in solid solution with titania and not enough surface vanadia is present to completely cover the exposed titania. The sig-

nificant loss in activity of the 700°C calcined sample cannot be totally accounted for by the four- to fivefold loss in surface area produced by the high calcination temperature, and must be partly due to the changes in the supported vanadia phase. This additional drop in activity is probably also associated with the incomplete monolayer of the surface vanadia since earlier studies also demonstrated that a partially covered titania support exhibits a substantial drop in activity for o-xylene oxidation (8, 9). Thus, it appears that the poor catalytic performance of the V$_2$O$_5$/TiO$_2$(anatase) catalyst calcined at 700°C is primarily a consequence of the formation of exposed titania sites in the incomplete monolayer of the surface vanadia at elevated temperatures.

The 7% V$_2$O$_5$/TiO$_2$ catalyst calcined at 700°C was impregnated with an additional 2% V$_2$O$_5$ and calcined at 450°C to investigate the above hypothesis that an incomplete monolayer of surface vanadia was responsible for the poor catalytic activity and selectivity. The objective of this second vanadia impregnation step was to cover the exposed titania sites, produced by the initial 700°C temperature treatment, with surface vanadia species. The resulting catalyst, 2% V$_2$O$_5$(7% V$_2$O$_5$/TiO$_2$—700°C) calcined at 450°C, remarkably improved the activity and selectivity of the V$_2$O$_5$/TiO$_2$ catalyst initially treated at 700°C. The C$_8$-oxygenate selectivity became comparable to that observed with the 7% V$_2$O$_5$/TiO$_2$ (anatase) catalysts calcined at lower temperatures. The addition of the vanadia also significantly increased the catalyst activity toward o-xylene oxidation. The activity, however, was still much lower than that observed for the 7% V$_2$O$_5$/TiO$_2$ (anatase) catalysts calcined at lower temperatures because of the four- to fivefold loss in surface area produced by the initial 700°C temperature treatment. Furthermore, this catalyst did not deactivate with time on stream and was stable throughout the run. This marked improvement of the V$_2$O$_5$/TiO$_2$ catalyst

calcined at 700°C is consistent with the above conclusion that the high-temperature treatment produces an incomplete monolayer of surface vanadia which is responsible for the extremely poor selectivity and activity of the catalyst toward o-xylene oxidation.

Gasior et al. observed that the degradation of the catalytic performance of V$_2$O$_5$/TiO$_2$(anatase) occurred even after a 600°C calcination (12). The V$_2$O$_5$/TiO$_2$(anatase) catalysts calcined at 600°C exhibited a significant drop in activity and gave extremely poor phthalic anhydride yields. For the 600°C calcined V$_2$O$_5$/TiO$_2$(anatase) catalysts not all the vanadia was incorporated into the titania lattice and supported crystalline V$_2$O$_5$ was still present (12). Yet, the catalytic performance of these V$_2$O$_5$/TiO$_2$ (anatase) catalysts for o-xylene oxidation was poor. This observation further confirms the earlier conclusion that crystalline V$_2$O$_5$ in V$_2$O$_5$/TiO$_2$ catalysts possesses a low activity for o-xylene oxidation (8, 9), and that the catalytic performance of V$_2$O$_5$/TiO$_2$(anatase) catalysts is related to the changes in the monolayer of surface vanadia on titania.

CONCLUSIONS

The state of V$_2$O$_5$/TiO$_2$(anatase) is strongly dependent on calcination temperature. In the presence of vanadia the TiO$_2$ (anatase) support exhibits a simultaneous loss in surface area and structural transformation to rutile at elevated calcination temperatures. The morphology of the supported vanadia phase also depends on calcination temperature. At low calcination temperatures, 110–200°C, the vanadia exists as vanadyl oxalate, the starting vanadia salt. At intermediate calcination temperatures 350–575°C, vanadia is present as a complete monolayer of surface vanadia species coordinated to the titania support and V$_2$O$_5$ crystallites. At a calcination temperature of 575°C and above the supported vanadia phase reacts with the TiO$_2$(anatase) support to yield V$_x$Ti$_{1-x}$O$_2$(rutile). These

structural changes have a pronounced effect on the catalytic performance of V_2O_5/TiO_2(anatase) catalysts for the oxidation of o-xylene. The optimum catalytic performance is observed for prolonged calcination at intermediate temperature, 350–575°C, where a complete monolayer of surface vanadia exists on the TiO_2(anatase) support. The complete monolayer of surface vanadia and crystalline vanadia phases remain intact during the o-xylene oxidation reaction and become partially reduced by the reaction environment. At very high calcination temperatures, the supported vanadia is present as crystalline $V_xTi_{1-x}O_2$ (rutile) and as an incomplete monolayer of surface vanadia species. The poor catalytic activity and selectivity of such a high-temperature-treated catalyst was dramatically improved by the formation of a complete monolayer of surface vanadia by the addition of more vanadia to the V_2O_5/TiO_2 sample.

ACKNOWLEDGMENTS

REFERENCES

1. VanHove, D., and Blanchard, M., *Bull. Sci. Chim. Fr.*, 3291 (1971).
2. Grabowski, R., Grzybowska, B., Haber, J., and Sloczynski, J., *React. Kinet. Catal. Lett.* 2, 81 (1975).
3. Bond, G. C., Sarkany, J., and Parfitt, G. D., *J. Catal.* 57, 476 (1979).
4. Murakami, Y., Inomata, M., Miyamoto, A., and Mori, K., *in* "Proceedings, 7th International Congress on Catalysis, Tokyo, 1980," p. 1344. Elsevier, Amsterdam, 1981.
5. Bond, G. C., and Konig, P., *J. Catal.* 77, 309 (1982).
6. Bond, G. C., and Bruckman, K., *Faraday Discuss.* 72, 235 (1981).
7. Van Hengstum, A. J., Van Ommen, J. G., Bosch, H., and Gellings, P. J., *Appl. Catal.* 8, 369 (1983).
8. Gasior, M., Gasior, I., and Grzybowska, B., *Appl. Catal.* 10, 87 (1984).
9. Wachs, I. E., Saleh, R. Y., Chan, S. S., and Chersich, C. C., *Appl. Catal.* 15, 339 (1985).
10. Roozeboom, F., Mittelmeijer-Hazeleger, M. C., Moulijn, J. A., Medema, J., de Beer, V. H. J., and Gellings, P. J., *J. Phys. Chem.* 84, 2783 (1980).
11. Kozlowski, R., Pettifer, R. F., and Thomas, J. M., *J. Phys. Chem.* 87, 5176 (1983).
12. Gasior, I., Gasior, M., Grzybowska, B., Kozlowski, R., and Sloczynski, J., *Bull. Acad. Pol. Sci. Ser. Sci. Chim.* 27, 829 (1979); Gasior, M., and Grzybowska, B., *Bull. Acad. Pol. Sci. Ser. Sci. Chim.* 27, 835 (1979).
13. Cole, D. J., Cullin, C. F., and Hucknall, D. J., *J. Chem. Soc.* 72, 2185 (1976).
14. Vejux, A., and Courtine, P., *J. Solid State Chem.* 23, 93 (1978); Courtine, P., and Vejux, A., *C. R. Acad. Sci. Paris Ser. C* 286, 135 (1978).
15. Dyrek, K., Serwicka, E., and Grzybowska, B., *React. Kinet. Catal. Lett.* 10, 93 (1979).
16. Wagner, C. D., Riggs, M. W., Davis, L. E., Moulder, J., and Muilenberg, G. E., "Handbook of X-Ray and Photoelectron Spectroscopy." Physical Electronics Industries, Eden Prairie, MN, 1979.
17. Chan, S. S., Wachs, I. E., Murrell, L. L., and Dispenziere, N. C., Jr., *J. Catal.* 92, 1 (1985).
18. Fuller, M. P., and Griffiths, P. R., *Anal. Chem.* 50, 1906 (1978).
19. Ng, K. Y. S., Zhou, X., and Gulari, E., to be published.
20. Beattie, I. R., and Gilson, T. R., *J. Chem. Soc.* (A), 2322 (1969); *Proc. R. Soc. London Ser. A* 307, 407 (1968).
21. Colton, R. J., Guzman, R. J., and Rabalais, J. W., *J. Appl. Phys.* 49, 409 (1978).
22. Wachs, I. E., Chan, S. S., and Saleh, R. Y., *J. Catal.* 91, 366 (1985).
23. Wachs, I. E., and Chan, S. S., to be published.
24. Soled, S., Murrell, L. L., Wachs, I. E., McVicker, G. B., Sherman, L. G., Chan, S., Dispenziere, N. C., and Baker, R. T. K., *in* "Solid State Chemistry in Catalysis" (R. K. Grasselli and J. F. Brazdil, Eds.), ACS Symp. Ser. 279 p. 165. Amer. Chem. Soc., Washington, D.C., 1985.
25. Yabrov, A. A., Ismailov, E. G., Boreskov, G. K., Ivanov, A. A., and Anufrenko, V. F., *React. Kinet. Catal. Lett.* 3, 237 (1975).